Field theoretic calculation of energy cascade rates in nonhelical magnetohydrodynamic turbulence

Mahendra K. Verma

Department of Physics, Indian Institute of Technology, Kanpur – 208016, INDIA
(Dated: October 19, 2002)

Energy cascade rates and Kolmogorov's constant for nonhelical steady magnetohydrodynamic turbulence have been calculated by solving the flux equations to the first order in perturbation. For zero cross helicity and space dimension $d = 3$, magnetic energy cascades from large length-scales to small length-scales (forward cascade). In addition, there are energy fluxes from large-scale magnetic field to small-scale velocity field, large-scale velocity field to small-scale magnetic field, and large-scale velocity field to large-scale magnetic field. Kolmogorov's constant for magnetohydrodynamics is approximately equal to that for fluid turbulence (≈ 1.6) for Alfvén ratio $0.5 \leq r_A \leq \infty$. For higher space-dimensions, the energy fluxes are qualitatively similar, and Kolmogorov's constant varies as $d^{1/3}$. For the normalized cross helicity $\sigma_c \to 1$, the cascade rates are proportional to $(1-\sigma_c)/(1+\sigma_c)$, and the Kolmogorov's constants vary significantly with σ_c.

I. INTRODUCTION

There are various phenomenological, numerical, and theoretical result on magnetohydrodynamics (MHD) turbulence. Kraichnan [1] and Irosnikov [2] proposed a first phenomenology for homogeneous and isotropic MHD which connects energy spectrum and cascade rates. In this phenomenology, the kinetic and magnetic energy spectrum ($E^u(k)$ and $E^b(k)$ respectively) are proportional to $k^{-3/2}$, and the energy cascade rate of flux $\Pi = (E(k))^2 k^3/B_0$, where B_0 is the mean magnetic field. In an alternate phenomenology, Marsch [3], Matthaeus and Zhou [4], and Zhou and Matthaeus [5] predicted that energy spectrum is Kolmogorov-like ($E(k) \propto k^{-5/3}$) and $\Pi = (E(k))^{3/2} k^{5/2}$. Verma et al. [6] numerically calculated the energy cascade rates of Elsässer variable $\mathbf{u} \pm \mathbf{b}$ ($\mathbf{u}, \mathbf{b}$ are velocity and magnetic field fluctuations), and found their results to be consistent with Kolmogorov-like phenomenology, rather that that of Kraichnan and Irosnikov. Frick and Sokoloff [7] studied the spectra and cascade rates in a shell model of MHD turbulence; they found the spectral index to be close to $5/3$ in absence of cross helicity and magnetic helicity. According to their study, the helicities suppress the cascade process. Recently, Müller and Biskamp [8] and Biskamp and Müller [9] computed the spectral index and found it to be closer to $5/3$. Kolmogorov-like spectrum is also supported by recent theoretical results [10, 11, 12, 13, 14, 15].

The energy cascade rates of MHD depend on cross helicity ($H_c = \mathbf{u} \cdot \mathbf{b}$), magnetic helicity ($H_M = \mathbf{a} \cdot \mathbf{b}$, where $\mathbf{a}$ is vector potential), and kinetic helicity ($H_K = \mathbf{u} \cdot \omega$, where ω is vorticity). Pouquet *et al.* [16] applied EDQNM approximation to study energy fluxes. For nonhelical MHD, Pouquet et al. [16] argued that the ME cascade is forward, i.e., from large-scale to small-scale. However, in the presence of helicity, they observed that the large-scale magnetic energy brings to equipartition the small-scale kinetic and magnetic excitation by Alfvén effect, and the "residual helicity", $H_K - H_M$, induces growth of large-scale magnetic energy and helicity. Pouquet and Patterson [17] studied this problem using direct numerical simulation and arrived at similar conclusions. In the present paper we will derive the energy fluxes of nonhelical MHD using field theoretic methods. The energy fluxes of helical MHD are discussed in a companion paper, Verma [18], referred to as paper II.

Since there are two fields $\mathbf{u}$ and $\mathbf{b}$ in MHD, the energy can be transferred from $\mathbf{u}$ to $\mathbf{u}$, $\mathbf{u}$ to $\mathbf{b}$, and $\mathbf{b}$ to $\mathbf{b}$. The resulting energy fluxes due to these transfers are illustrated in Fig. 1. These fluxes have been numerically calculated recently by Dar *et al.* [19] and Ishizawa and Hattori [20] for two-dimensional (2D) MHD turbulence. The numerical values calculated by Dar *et al.* for $\sigma_c \approx 0$ and r_A (KE/ME) ≈ 0.5 are listed in Table I. The prime conclusions of Dar *et al.* [19] and Ishizawa and Hattori's [20] 2D numerical study are: (1) the ME cascades from large-scales to small-scales (forward cascade); (2) there is a significant energy transfer from large length-scale velocity field to large length-scale magnetic field; this transfer could play an important role in ME enhancement; (3) there is an inverse cascade of KE. In another recent work, Cho and Vishniac [21] have derived some interesting scaling relationships between the energy transfer rates and verified them using numerical simulations. Since the direction of total energy cascade is the same in 2D and 3D (three-dimensional) MHD turbulence, some of the conclusions drawn by Dar *et al.* [19] and Ishizawa and Hattori [20] based on 2D simulations are expected to hold at least qualitatively in 3D MHD turbulence. Therefore, in this paper we compare the numerical results of Dar et al. [19] and Ishizawa and Hattori [20] with our 3D analytic results.

In the present paper we have carried out the energy cascade rate calculation for MHD turbulence for the *inertial-*

range wavenumbers using perturbative field-theoretic technique. Here we assume that the turbulence is homogeneous and isotropic to make the problem tractable. Even though the real-world turbulence does not satisfy these properties, at least at the large-scales, many conclusions drawn using this assumption give us important insights into the energy transfer mechanisms, as will be discussed in this paper and paper II. We assume that the mean magnetic field is absent; this assumption is to ensure that the turbulence is isotropic. Our procedure requires Fourier space integrations of functions involving products of energy spectrum and the Greens functions. Since there is a general agreement on Kolmogorov-like spectrum for MHD turbulence, we take $E(k) \propto k^{-5/3}$ for all the energy spectra for MHD. For the Greens function, we substitute the "renormalized" or "dressed" Greens function computed by Verma [14]. After this substitution, various energy fluxes and Kolmogorov's constant of MHD are computed. Using the steady-state condition, we also calculate the energy supply from the large-scale velocity field to the large-scale magnetic field. This result is quite robust, and is independent of the nature of large-scale forcing. In this paper we assume both kinetic and magnetic helicity to be absent. The energy fluxes for helical MHD are discussed in paper II.

The parameter space of MHD is rather large because of various energy spectra. The two well known parameters are: the normalized cross helicity σ_c, which is the ratio of twice cross helicity and energy; and the Alfvén ratio r_A, which is the ratio of kinetic energy and magnetic energy. Calculation of cascade rates for arbitrary σ_c and r_A is quite complex. In this paper we limit ourselves to two limiting cases: (1) $\sigma_c = 0$ and whole range of r_A; (2) $\sigma_c \to 1$ and $r_A = 1$. Strictly speaking, the parameters used in our calculations are spectral $\sigma_c(k) = 2H_c(k)/(E^u(k) + E^b(k))$ and $r_A(k) = E^u(k)/E^b(k)$. Since our calculation is confined to inertial-range wavenumbers where Kolmogorov's 5/3 powerlaw is valid for all the energy spectra of MHD, both $\sigma(k)$ and $r_A(k)$ can be treated as constants. Note that these parameters may differ from the global σ_c and r_A. We carry out our theoretical analysis in various dimensions. We will show that our theoretical results are in general agreement with the simulation results of Dar *et al.* [19] and Ishizawa and Hattori [20].

The outline of this paper is as follows: In section 2 we calculate various cascade rates for $\sigma_c = 0$ case. The other extreme case $\sigma_c \to 1$ is considered in section 3. Section 4 contains summary and conclusions.

II.   CASCADE RATES IN MHD TURBULENCE: $\sigma_c = 0$

In this section we will analytically compute the energy cascade rates when $\sigma_c = 0$. We take the following form of Kolmogorov's spectrum for kinetic energy (KE) and magnetic energy (ME)

$$E^u(k) = K^u \Pi^{2/3} k^{-5/3} \tag{1}$$
$$E^b(k) = E^u(k)/r_A \tag{2}$$

where K^u is Kolmogorov's constant for MHD turbulence, and Π is the total energy flux. Another Kolmogorov's constant K is defined for the total energy,

$$E_{total}(k) = E^u(k) + E^b(k) = E(k) = K\Pi^{2/3}k^{-5/3}, \tag{3}$$

with

$$K = K^u(1 + r_A^{-1}) \tag{4}$$

With this preliminaries we start our flux calculation.

The incompressible MHD equations are

$$\frac{\partial \mathbf{u}}{\partial t} + (\mathbf{u} \cdot \nabla)\mathbf{u} = -\nabla p + (\mathbf{b} \cdot \nabla)\mathbf{b} + \nu\nabla^2\mathbf{u} \tag{5}$$

$$\frac{\partial \mathbf{b}}{\partial t} + (\mathbf{u} \cdot \nabla)\mathbf{b} = -(\mathbf{b} \cdot \nabla)\mathbf{u} + \eta\nabla^2\mathbf{b} \tag{6}$$

$$\nabla \cdot \mathbf{u} = 0 \tag{7}$$
$$\nabla \cdot \mathbf{b} = 0 \tag{8}$$

where $\mathbf{u}$ and $\mathbf{b}$ are the velocity and magnetic fields respectively, p is the total pressure, and ν and μ are the kinematic viscosity and magnetic diffusivity respectively. To compute various energy transfers among various Fourier modes we resort to the energy equations, which are [16, 19, 22]

$$\left(\frac{\partial}{\partial t} + 2\nu k^2\right) C^{uu}(\mathbf{k}, t, t) = \frac{1}{(d-1)(2\pi)^d} \int_{\mathbf{k'}+\mathbf{p}+\mathbf{q}=\mathbf{0}} \frac{d\mathbf{p}}{(2\pi)^d} [S^{uu}(\mathbf{k'}|\mathbf{p}|\mathbf{q}) + S^{uu}(\mathbf{k'}|\mathbf{q}|\mathbf{p})]$$

$$+S^{ub}(\mathbf{k'}|\mathbf{p}|\mathbf{q}) + S^{ub}(\mathbf{k'}|\mathbf{q}|\mathbf{p})] \tag{9}$$

$$\left(\frac{\partial}{\partial t} + 2\eta k^2\right) C^{bb}(\mathbf{k}, t, t) = \frac{1}{(d-1)(2\pi)^d} \int_{\mathbf{k'}+\mathbf{p}+\mathbf{q}=\mathbf{0}} \frac{d\mathbf{p}}{(2\pi)^d} [S^{bu}(\mathbf{k'}|\mathbf{p}|\mathbf{q}) + S^{bu}(\mathbf{k'}|\mathbf{q}|\mathbf{p})$$

$$+S^{bb}(\mathbf{k'}|\mathbf{p}|\mathbf{q}) + S^{bb}(\mathbf{k'}|\mathbf{q}|\mathbf{p})] \tag{10}$$

The above integrals have constraints that $\mathbf{k'} + \mathbf{p} + \mathbf{q} = \mathbf{0}$ ($\mathbf{k} = -\mathbf{k'}$). The equal-time correlation functions used in the energy equations are defined using

$$\langle u_i(\mathbf{p}, t) u_j(\mathbf{q}, t) \rangle = P_{ij}(\mathbf{p}) C^{uu}(\mathbf{p}, t, t) \delta(\mathbf{p} + \mathbf{q}) \tag{11}$$

$$\langle b_i(\mathbf{p}, t) b_j(\mathbf{q}, t) \rangle = P_{ij}(\mathbf{p}) C^{bb}(\mathbf{p}, t, t) \delta(\mathbf{p} + \mathbf{q}) \tag{12}$$

$$\langle u_i(\mathbf{p}, t) b_j(\mathbf{q}, t) \rangle = P_{ij}(\mathbf{p}) C^{ub}(\mathbf{p}, t, t) \delta(\mathbf{p} + \mathbf{q}) \tag{13}$$

and the energy transfer rates $S(\mathbf{k'}|\mathbf{p}|\mathbf{q})$ are defined using

$$S^{uu}(\mathbf{k'}|\mathbf{p}|\mathbf{q}) = -\Im([\mathbf{k'} \cdot \mathbf{u}(\mathbf{q})][\mathbf{u}(\mathbf{k'}) \cdot \mathbf{u}(\mathbf{p})]), \tag{14}$$

$$S^{bb}(\mathbf{k'}|\mathbf{p}|\mathbf{q}) = -\Im([\mathbf{k'} \cdot \mathbf{u}(\mathbf{q})][\mathbf{b}(\mathbf{k'}) \cdot \mathbf{b}(\mathbf{p})]), \tag{15}$$

$$S^{ub}(\mathbf{k'}|\mathbf{p}|\mathbf{q}) = \Im([\mathbf{k'} \cdot \mathbf{b}(\mathbf{q})][\mathbf{u}(\mathbf{k'}) \cdot \mathbf{b}(\mathbf{p})]), \tag{16}$$

$$S^{bu}(\mathbf{k'}|\mathbf{p}|\mathbf{q}) = -S^{ub}(\mathbf{p}|\mathbf{k'}|\mathbf{q}) \tag{17}$$

Here $\Im$ stands for the imaginary part of the argument. Note that $C^{ub} = 0$ because σ_c has been taken to be zero. The above equations are based on Dar et al.'s formalism, which is a generalization of those of Pouquet *et al.* [16] and Stanišić [22] and others. In Dar *et al.*'s formalism, the terms $S(\mathbf{k}|\mathbf{p}|\mathbf{q})$ represents energy transfer from mode $\mathbf{p}$ (the second argument of S) to $\mathbf{k}$ (the first argument of S) with mode $\mathbf{q}$ (the third argument of S) acting as a mediator. Note that in the expression for S, the field variables with the first and second arguments are dotted together, while the field variables with the third argument is dotted with the wavevector $\mathbf{k}$. Dar *et al.*'s formulas has certain advantages over those of Pouquet *et al.* [16] and Stanišić [22]. Some of the quantities to be defined below were not accessible in the earlier formalism, but now they can be calculated using Dar *et al.*'s formulas. In addition, the flux formulas derived using the new scheme are relatively simpler.

After some algebraic manipulation it can be shown that

$$S^{uu}(\mathbf{k'}|\mathbf{p}|\mathbf{q}) + S^{uu}(\mathbf{k'}|\mathbf{q}|\mathbf{p}) + S^{uu}(\mathbf{p}|\mathbf{k'}|\mathbf{q}) + S^{uu}(\mathbf{p}|\mathbf{q}|\mathbf{k'}) + S^{uu}(\mathbf{q}|\mathbf{k'}|\mathbf{p}) + S^{uu}(\mathbf{q}|\mathbf{p}|\mathbf{k'}) = 0 \tag{18}$$

$$S^{bb}(\mathbf{k'}|\mathbf{p}|\mathbf{q}) + S^{bb}(\mathbf{k'}|\mathbf{q}|\mathbf{p}) + S^{bb}(\mathbf{p}|\mathbf{k'}|\mathbf{q}) + S^{bb}(\mathbf{p}|\mathbf{q}|\mathbf{k'}) + S^{bb}(\mathbf{q}|\mathbf{k'}|\mathbf{p}) + S^{bb}(\mathbf{q}|\mathbf{p}|\mathbf{k'}) = 0 \tag{19}$$

$$S^{ub}(\mathbf{k'}|\mathbf{p}|\mathbf{q}) + S^{ub}(\mathbf{k'}|\mathbf{q}|\mathbf{p}) + S^{ub}(\mathbf{p}|\mathbf{k'}|\mathbf{q}) + S^{ub}(\mathbf{p}|\mathbf{q}|\mathbf{k'}) + S^{ub}(\mathbf{q}|\mathbf{k'}|\mathbf{p}) + S^{ub}(\mathbf{q}|\mathbf{p}|\mathbf{k'})$$

$$+S^{bu}(\mathbf{k'}|\mathbf{p}|\mathbf{q}) + S^{bu}(\mathbf{k'}|\mathbf{q}|\mathbf{p}) + S^{bu}(\mathbf{p}|\mathbf{k'}|\mathbf{q}) + S^{bu}(\mathbf{p}|\mathbf{q}|\mathbf{k'}) + S^{bu}(\mathbf{q}|\mathbf{k'}|\mathbf{p}) + S^{bu}(\mathbf{q}|\mathbf{p}|\mathbf{k'}) = 0 \tag{20}$$

These are the statements of "detailed conservation of energy" in MHD triads (when $\nu = \eta = 0$) [23].

For energy flux study, we split the wavenumber space into two regions: $k < k_0$ (inside "k_0-sphere") and $k > k_0$ (outside "k_0-sphere"). This division is done for both velocity and magnetic fields. The energy transfer could take place from inside/outside u/b-sphere to inside/outside u/b-sphere. In terms of S, the energy flux from inside of the X-sphere to outside of the Y-sphere is

$$\Pi_{Y>}^{X<}(k_0) = \int_{k'>k_0} \frac{d\mathbf{k}}{(2\pi)^d} \int_{p<k_0} \frac{d\mathbf{p}}{(2\pi)^d} \left\langle S^{YX}(\mathbf{k'}|\mathbf{p}|\mathbf{q}) \right\rangle \tag{21}$$

where X and Y stand for u or b. The energy fluxes from inside u/b-sphere to outside u/b-sphere can be calculated by earlier formalism, as well as that of Dar *et al.* However, the fluxes from inside u-sphere to inside b-sphere, and outside u-sphere to outside b-sphere can be numerically calculated only by Dar *et al.*'s formalism. In this paper we will analytically calculate the above fluxes in the inertial range using the Kolmogorov-like energy spectrum.

We assume that the kinetic energy is forced at small wavenumbers, and the turbulence is steady. Therefore,

$$\Pi_{b<}^{u<} = \Pi_{b>}^{b<} + \Pi_{u>}^{b<} \tag{22}$$

$$\text{Input Kinetic Energy} = \Pi_{u>}^{u<} + \Pi_{b>}^{u<} + \Pi_{b<}^{u<} \tag{23}$$

We calculate the energy flux $\Pi_{b<}^{u<}$ using the above steady-state property. Hence the energy feed into the large-scale magnetic field from the large-scale velocity field could be obtained theoretically irrespective of nature of large-scale forcing.

We will analytically calculate the above energy fluxes [Eq. (21)] in the inertial range to the leading order in perturbation series. It is assumed that $\mathbf{u}(\mathbf{k})$ is gaussian to leading order. Consequently, the ensemble average of S^{YX}, $\langle S^{YX} \rangle$, is zero to the zeroth order, but is nonzero to the first order. The first order terms for $S^{YX}(k|p|q)$ in terms of Feynman diagrams are shown below:

$$\langle S^{uu}(k'|p|q)\rangle \;=\; \qquad\qquad + \qquad\qquad + \qquad\qquad ; \qquad\qquad (24)$$

$$-\langle S^{ub}(k'|p|q)\rangle \;=\; - \qquad\qquad + \qquad\qquad + \qquad\qquad ; \qquad\qquad (25)$$

$$-\langle S^{bu}(k'|p|q)\rangle \;=\; \qquad\qquad - \qquad\qquad + \qquad\qquad ; \qquad\qquad (26)$$

$$\langle S^{bb}(k'|p|q)\rangle \;=\; \qquad\qquad + \qquad\qquad - \qquad\qquad \qquad\qquad (27)$$

In the above diagrams the solid, dashed, wiggly (photon), and curly (gluons) lines denote $\langle u_i u_j \rangle$, $\langle b_i b_j \rangle$, G^{uu}, and G^{bb} respectively. In all the diagrams, the left vertex denotes k_i, while the filled circle and the empty circles of right vertex represent $(-i/2)P^+_{ijm}$ and $-iP^-_{ijm}$ respectively. Since G^{ub}, G^{bu}, C^{ub}, and C^{bu} are zero when $\sigma_c = 0$, we have not included the Feynman diagrams containing these terms. When we substitute $\langle u_i u_j \rangle$, $\langle b_i b_j \rangle$ using Eqs. (11,12), we obtain terms involving $C^X(p,t,t')C^Y(q,t,t')$. The resulting expressions for various $\langle S^{YX}(k|p|q)\rangle$ are

$$
\begin{aligned}
\langle S^{uu}(k|p|q)\rangle \;=\; &\int_{-\infty}^{t} dt' [T_1(k,p,q)G^{uu}(k,t-t')C^{uu}(p,t,t')C^{uu}(q,t,t') \\
&+T_5(k,p,q)G^{uu}(p,t-t')C^{uu}(k,t,t')C^{uu}(q,t,t') \\
&+T_9(k,p,q)G^{uu}(q,t-t')C^{uu}(k,t,t')C^{uu}(p,t,t')]
\end{aligned}
\qquad (28)
$$

$$
\begin{aligned}
\langle S^{ub}(k|p|q)\rangle \;=\; -&\int_{-\infty}^{t} dt' [T_2(k,p,q)G^{uu}(k,t-t')C^{bb}(p,t,t')C^{bb}(q,t,t') \\
&+T_7(k,p,q)G^{bb}(p,t-t')C^{uu}(k,t,t')C^{bb}(q,t,t') \\
&+T_{11}(k,p,q)G^{uu}(q,t-t')C^{uu}(k,t,t')C^{bb}(p,t,t')]
\end{aligned}
\qquad (29)
$$

$$
\begin{aligned}
\langle S^{bu}(k|p|q)\rangle \;=\; -&\int_{-\infty}^{t} dt' [T_3(k,p,q)G^{bb}(k,t-t')C^{uu}(p,t,t')C^{bb}(q,t,t') \\
&+T_6(k,p,q)G^{uu}(p,t-t')C^{bb}(k,t,t')C^{bb}(q,t,t') \\
&+T_{12}(k,p,q)G^{bb}(q,t-t')C^{bb}(k,t,t')C^{uu}(p,t,t')]
\end{aligned}
\qquad (30)
$$

$$\langle S^{bb}(k|p|q)\rangle = \int_{-\infty}^{t} dt' [T_4(k,p,q)G^{bb}(k,t-t')C^{bb}(p,t,t')C^{uu}(q,t,t')$$

$$+T_8(k,p,q)G^{bb}(p,t-t')C^{bb}(k,t,t')C^{uu}(q,t,t')$$
$$+T_{10}(k,p,q)G^{uu}(q,t-t')C^{bb}(k,t,t')C^{bb}(p,t,t')] \tag{31}$$

where $T_i(k,p,q)$ are functions of wavevectors k,p, and q given in Appendix A.

The Greens functions can be written in terms of "effective" or "renormalized" viscosity $\nu(k)$ and resistivity $\eta(k)$ (see Verma [14] for details) as

$$G^{uu}(k,t-t') = \exp\left(-\nu(k)k^2(t-t')\right) \tag{32}$$
$$G^{bb}(k,t-t') = \exp\left(-\eta(k)k^2(t-t')\right) \tag{33}$$

The relaxation time for $C^{uu}(k,t,t')$ is assumed to be the same as that of G^{uu}, and that of $C^{bb}(k,t,t')$ is assumed to be the same as that of G^{bb}. Therefore the time dependence of the unequal-time correlation functions will be

$$C^{uu}(k,t,t') = \exp\left(-\nu(k)k^2(t-t')\right)C^{uu}(k,t,t) \tag{34}$$
$$C^{bb}(k,t,t') = \exp\left(-\eta(k)k^2(t-t')\right)C^{bb}(k,t,t) \tag{35}$$

The above forms of Green's and correlation functions are substituted in the expression of $\langle S^{YX}\rangle$, and the t' integral is performed. Now Eqs. (21, 28) yield the following flux formula for $\Pi_{u>}^{u<}(k_0)$:

$$\Pi_{u>}^{u<}(k_0) = \int_{k>k_0} \frac{d\mathbf{k}}{(2\pi)^d} \int_{p<k_0} \frac{d\mathbf{p}}{(2\pi)^d} \frac{1}{\nu(k)k^2 + \nu(p)p^2 + \nu(q)q^2} \times$$
$$[T_1(k,p,q)C^{uu}(p)C^{uu}(q) + T_5(k,p,q)C^{uu}(k)C^{uu}(q) + T_9(k,p,q)C^{uu}(k)C^{uu}(p)] \tag{36}$$

The expressions for the other fluxes can be obtained similarly.

The equal-time correlation functions $C^{uu}(k,t,t)$ and $C^{bb}(k,t,t)$ at the steady-state can be written in terms of one dimensional energy spectrum as

$$C^{uu}(k,t,t) = \frac{2(2\pi)^d}{S_d(d-1)} k^{-(d-1)} E^u(k) \tag{37}$$

$$C^{bb}(k,t,t) = \frac{2(2\pi)^d}{S_d(d-1)} k^{-(d-1)} E^b(k) \tag{38}$$

where S_d is the surface area of d-dimensional unit spheres. We are interested in the fluxes in the inertial range. Therefore, we substitute Kolmogorov's spectrum [Eqs. (1,2)] for the energy spectrum. The effective viscosity and resistivity are proportional to $k^{-4/3}$, i.e.,

$$\nu(k) = (K^u)^{1/2}\Pi^{1/3}k^{-4/3}\nu^* \tag{39}$$
$$\eta(k) = (K^u)^{1/2}\Pi^{1/3}k^{-4/3}\eta^*. \tag{40}$$

and the parameters ν^* and η^* were calculated in Verma [14].

The d-dimensional volume integral under the constraint $\mathbf{k}' + \mathbf{p} + \mathbf{q} = \mathbf{0}$ is given by [24]

$$\int_{\mathbf{p}+\mathbf{q}=\mathbf{k}} d\mathbf{q} = S_{d-1} \int dp dq \left(\frac{pq}{k}\right)^{d-2} (\sin\alpha)^{d-3} \tag{41}$$

where α is angle between vectors $\mathbf{p}$ and $\mathbf{q}$. We also nondimensionalize Eq. (36) by substituting [23]

$$k = \frac{k_0}{u}; \qquad p = \frac{k_0}{u}v; \qquad q = \frac{k_0}{u}w \tag{42}$$

which yields

$$\Pi_{Y>}^{X<} = (K^u)^{3/2}\Pi \left[\frac{4S_{d-1}}{(d-1)^2 S_d} \int_0^1 dv \ln(1/v) \int_{1-v}^{1+v} dw(vw)^{d-2}(\sin\alpha)^{d-3}F_{Y>}^{X<}(v,w)\right] \tag{43}$$

where the integrals $F_{Y>}^{X<}(v,w)$ are

$$F_{u>}^{u<} = \frac{1}{\nu^*(1+v^{2/3}+w^{2/3})}[t_1(v,w)(vw)^{-d-\frac{2}{3}}+t_5(v,w)w^{-d-\frac{2}{3}}+t_9(v,w)v^{-d-\frac{2}{3}}] \tag{44}$$

$$F_{u>}^{b<} = \frac{-1}{\nu^*+\eta^*(v^{2/3}+w^{2/3})}[t_2(v,w)(vw)^{-d-\frac{2}{3}}r_A^{-2}+t_7(v,w)w^{-d-\frac{2}{3}}r_A^{-1}+t_{11}(v,w)v^{-d-\frac{2}{3}}r_A^{-1}] \tag{45}$$

$$F_{b>}^{u<} = \frac{-1}{\nu^*v^{2/3}+\eta^*(1+w^{2/3})}[t_3(v,w)(vw)^{-d-\frac{2}{3}}r_A^{-1}+t_6(v,w)w^{-d-\frac{2}{3}}r_A^{-2}+t_{12}(v,w)v^{-d-\frac{2}{3}}r_A^{-1}] \tag{46}$$

$$F_{b>}^{b<} = \frac{1}{\nu^*w^{2/3}+\eta^*(1+v^{2/3})}[t_4(v,w)(vw)^{-d-\frac{2}{3}}r_A^{-1}+t_8(v,w)w^{-d-\frac{2}{3}}r_A^{-1}+t_{10}(v,w)v^{-d-\frac{2}{3}}r_A^{-2}]. \tag{47}$$

Here $t_i(v,w) = T_i(k,kv,kw)/k^2$. Note that the energy fluxes are constant consistent with the Kolmogorov's picture. We compute the bracketed terms (denoted by $I_{Y>}^{X<}$) numerically and find that all of them converge. Let us denote $I = I_{u>}^{u<} + I_{u>}^{b<} + I_{b>}^{u<} + I_{b>}^{b<}$. Using the fact that the total flux Π is

$$\Pi = \Pi_{u>}^{u<} + \Pi_{u>}^{b<} + \Pi_{b>}^{u<} + \Pi_{b>}^{b<}, \tag{48}$$

we can calculate the value of constant K^u, which is

$$K^u = (I)^{-2/3} \tag{49}$$

In addition, the energy flux ratios can be computed using $\Pi_{Y>}^{X<}/\Pi = I_{Y>}^{X<}/I$. The flux ratio $\Pi_{b<}^{u<}/\Pi$ is obtained using steady-state condition [Eq. (22)]. The values of constant K can be computed using Eq. (4). The flux ratios and Kolmogorov's constants for $d=3$ and various r_A are listed in Table II. The same quantities for $r_A=1$ and various space dimensions are listed in Table III.

The following trends can be inferred by studying Table II. We find that for $d=3$, $\Pi_{u>}^{u<}/\Pi$ starts from 1 for large r_A and decreases nearly to zero near $r_A=0.3$. All other fluxes start from zero and increase up to some saturated values; this implies that near $r_A\approx1$, all the energy fluxes become significant. Clearly, the sign of $\Pi_{b>}^{b<}$ is positive, indicating that ME cascades from large length-scale to small length-scale. Under steady-state the large-scale ME is maintained by $\Pi_{b<}^{u<}$, which is one of the most dominant transfers near $r_A=0.5$. The energy flux $\Pi_{b<}^{u<}$ entering the large scales magnetic energy could play an important role in the amplification of magnetic energy. In paper II we will construct a dynamo model based on the energy fluxes.

The Kolmogorov constant K for $d=3$ is listed in Table II. For all r_A greater than 0.5, K is approximately constant and is close to 1.6, same as that for fluid turbulence ($r_A=\infty$). Since $\Pi\propto K^{-3/2}$, we can conclude that the variation of r_A (redistribution of fluid and magnetic energy, keeping the total energy fixed) does not change the total cascade rate. Near $r_A=0.3$, the constant K appears to increase, indicating a sudden drop in the cascade rate. When r_A is decreased further, near $r_A=0.25$ both $\nu^*\approx0$ and $\eta^*\approx0$ [14], or $K\to\infty$. This signals an absence of turbulence for r_A near 0.25. This is consistent with the fact that MHD equations are linear in the $r_A\to0$ (fully magnetic) limit, hence do not exhibit turbulence. However, it is still surprising that turbulence disappears near $r_A=0.25$ itself.

The Kolmogorov's constant K computed above can be used to estimate the amount of turbulent heating in the solar wind. Verma et al. [25] and Tu [26] have put constraints on the turbulent heating in the solar wind from the radial variation of temperature in the solar wind. Verma *et al.* [25] observed that when $K\approx1$, all the heating in the solar wind for streams with $\sigma_c\approx0$ can be accounted for by the turbulent heating. Our theoretical value for this constant in the absence of mean magnetic field is approximately 1.5, larger than 1. If we take $K\approx1.5$ for solar wind streams with $\sigma_c\approx0$, only a fraction, possibly around half $((1/1.5)^{3/2})$, of the heating will be due to turbulence. However, neglect of mean magnetic field, anisotropy, helicities etc. are gross assumptions, and we can only claim general consistency of the theoretical estimates with the observational results of the solar wind.

We have calculated the flux ratios and the constant K for various space dimensions $d\geq2.2$. In Verma [14] it has been shown that for $d<2.2$, the RG fixed point is unstable, and the renormalized parameters could not be determined. Due to that reason we have calculated fluxes and Kolmogorov's constant for $d\geq2$ only. For these calculations we take $r_A=1$, which is a generic case. The calculated values are shown in Table III. It is striking that all the fluxes are approximately the same for large d. In addition, $\Pi_{b<}^{u<}/\Pi$ is approximately 0.5 for all dimensions greater than 4.

We verify that $I_{Y>}^{X<}$ for constant ν^* and η^* are proportional to d^{-1}. In Verma [14] we find that $\nu^*,\eta^*\propto d^{-1/2}$. Therefore, $K\propto d^{-1/3}$. This result is a generalization of theoretical analysis of Fournier *et al.* [24] for fluid turbulence.

In this section we calculated the cascade rates for $\sigma_c=0$. In the next section we take the other limit $\sigma_c\to1$.

III. CASCADE RATES IN MHD TURBULENCE: $\sigma_c \to 1$

In this section we will describe the calculation of the energy cascade rates for the large normalized cross-helicity ($\sigma_c \to 1$), and show that the cascade rates crucially depend on cross helicity. For cases with $\sigma_c \to 1$, it is best to work with Elsässer variables $\mathbf{z}^\pm = \mathbf{u} \pm \mathbf{b}$. For the following discussion we will denote the ratio $\langle |z^-|^2 \rangle / \langle |z^+|^2 \rangle$ by r. Clearly $r \ll 1$. Here we limit ourselves to $r_A = 1$.

The incompressible MHD equations in terms of $\mathbf{z}^\pm$ are

$$\frac{\partial \mathbf{z}^\pm}{\partial t} + (\mathbf{z}^\mp \cdot \nabla)\mathbf{z}^\pm = -\nabla p + \nu_+ \nabla^2 \mathbf{z}^\pm + \nu_- \nabla^2 \mathbf{z}^\mp \tag{50}$$

$$\nabla \cdot \mathbf{z}^\pm = 0 \tag{51}$$

where p is the total pressure, and $\nu_\pm = (\nu \pm \eta)/2$. Numerical simulations of Verma et al. [27] and Dar [28], solar wind observations of Matthaeus and Goldstein [29], and Marsch and Tu [30], and theoretical calculations of Verma [13, 14] show that Kolmogorov-like energy spectrum is valid even for nonzero cross helicity, i.e.,

$$E^\pm(k) = K^\pm \frac{(\Pi^\pm)^{4/3}}{(\Pi^\mp)^{2/3}} k^{-5/3} \tag{52}$$

where $K^\pm$ are Kolmogorov's constants for MHD. The above equation was first derived by Marsch [3].

The corresponding equations for the energy evolution are

$$\left(\frac{\partial}{\partial t} + 2\nu_+ k^2\right) C^{\pm\pm}(\mathbf{k}, t, t) + 2\nu_- k^2 C^{\pm\mp}(\mathbf{k}, t, t) = \frac{1}{(d-1)(2\pi)^d} \int_{\mathbf{k}'+\mathbf{p}+\mathbf{q}=0} \frac{d\mathbf{p}}{(2\pi)^d}$$
$$[S^{\pm\pm}(\mathbf{k}'|\mathbf{p}|\mathbf{q}) + S^{\pm\pm}(\mathbf{k}'|\mathbf{q}|\mathbf{p})] \tag{53}$$

where

$$S^{\pm\pm}(\mathbf{k}'|\mathbf{p}|\mathbf{q}) = -\Im([\mathbf{k}' \cdot \mathbf{z}^\mp(\mathbf{q})][\mathbf{z}^\pm(\mathbf{k}') \cdot \mathbf{z}^\pm(\mathbf{p})]) \tag{54}$$

and the equal-time correlations functions $C^{\pm\pm}$ and $C^{\pm\mp}$ are defined using

$$\left\langle z_i^\pm(\mathbf{p}, t) z_j^\pm(\mathbf{q}, t) \right\rangle = P_{ij}(\mathbf{p}) C^{\pm\pm}(\mathbf{p}, t, t) \delta(\mathbf{p} + \mathbf{q}) \tag{55}$$

$$\left\langle z_i^\pm(\mathbf{p}, t) z_j^\mp(\mathbf{q}, t) \right\rangle = P_{ij}(\mathbf{p}) C^{\pm\mp}(\mathbf{p}, t, t) \delta(\mathbf{p} + \mathbf{q}) \tag{56}$$

From Eq. (54) it is evident that in the nonlinear transfers, the modes z^+ transfer energy only to z^+ while z^- acts as a mediator. Similarly z^- transfers energy only to z^- with z^+ acting as a mediator. It can be easily shown that

$$S^\pm(\mathbf{k}'|\mathbf{p}|\mathbf{q}) + S^\pm(\mathbf{k}'|\mathbf{q}|\mathbf{p}) + S^\pm(\mathbf{p}|\mathbf{k}'|\mathbf{q}) + S^\pm(\mathbf{p}|\mathbf{q}|\mathbf{k}') + S^\pm(\mathbf{q}|\mathbf{k}'|\mathbf{p}) + S^\pm(\mathbf{q}|\mathbf{p}|\mathbf{k}') = 0 \tag{57}$$

These equations correspond to the "detailed conservation of energy" in MHD triads.

In terms of $z^\pm$ variables, there are only two types of fluxes $\Pi^\pm$, one for the z^+ cascade and the other for z^- cascade. In terms of S, these energy fluxes $\Pi^\pm$ are

$$\Pi^\pm(k_0) = \int_{k'>k_0} \frac{d\mathbf{k}}{(2\pi)^d} \int_{p<k_0} \frac{d\mathbf{p}}{(2\pi)^d} \left\langle S^{\pm\pm}(\mathbf{k}'|\mathbf{p}|\mathbf{q}) \right\rangle \tag{58}$$

As described in the last section, the above fluxes are calculated to the leading order in perturbation series. To the first order, $\langle S^{\pm\pm}(\mathbf{k}'|\mathbf{p}|\mathbf{q}) \rangle$ are

$$\left\langle S^{\pm\pm}(k|p|q) \right\rangle = \int_{-\infty}^{t} dt'[T_{13}(k,p,q) G^{\pm\pm}(k, t-t') C^{\pm\mp}(p,t,t') C^{\mp\pm}(q,t,t')$$
$$+ T_{14}(k,p,q) G^{\pm\pm}(k,t-t') C^{\pm\pm}(p,t,t') C^{\mp\mp}(q,t,t')$$
$$+ T_{15}(k,p,q) G^{\pm\mp}(k,t-t') C^{\pm\pm}(p,t,t') C^{\mp\mp}(q,t,t')$$
$$+ T_{16}(k,p,q) G^{\pm\mp}(k,t-t') C^{\pm\mp}(p,t,t') C^{\mp\pm}(q,t,t')$$
$$+ T_{17}(k,p,q) G^{\pm\pm}(p,t-t') C^{\pm\mp}(k,t,t') C^{\mp\pm}(q,t,t')$$
$$+ T_{18}(k,p,q) G^{\pm\mp}(p,t-t') C^{\pm\pm}(k,t,t') C^{\mp\mp}(q,t,t')$$

$$+T_{19}(k,p,q)G^{\pm\mp}(p,t-t')C^{\pm\pm}(k,t,t')C^{\mp\mp}(q,t,t')$$
$$+T_{20}(k,p,q)G^{\pm\mp}(p,t-t')C^{\pm\pm}(k,t,t')C^{\mp\mp}(q,t,t')$$
$$+T_{21}(k,p,q)G^{\mp\pm}(q,t-t')C^{\pm\mp}(k,t,t')C^{\pm\pm}(p,t,t')$$
$$+T_{22}(k,p,q)G^{\mp\pm}(q,t-t')C^{\pm\pm}(k,t,t')C^{\pm\mp}(p,t,t')$$
$$+T_{23}(k,p,q)G^{\mp\mp}(q,t-t')C^{\pm\pm}(k,t,t')C^{\pm\mp}(p,t,t')$$
$$+T_{24}(k,p,q)G^{\mp\mp}(q,t-t')C^{\pm\mp}(k,t,t')C^{\pm\pm}(p,t,t')] \tag{59}$$

where $T_i(k,p,q)$ are given in Appendix A.

Now we use the approximation that r is small. In terms of renormalized $\hat{\nu}$ matrix

$$\hat{\nu}(k) = \begin{pmatrix} r\zeta & \alpha \\ r\psi & \beta \end{pmatrix}, \tag{60}$$

the Green's function $\hat{G}(k,t-t') = \exp -[\hat{\nu}k^2(t-t')]$ to leading order in r is

$$\hat{G}(k,t-t') = \begin{pmatrix} 1 - \frac{r\alpha\psi}{\beta^2}(1-e^{-\beta(t-t')}) & -\left\{\frac{\alpha}{\beta} + \frac{r\alpha}{\beta}\left(\frac{\zeta}{\beta} - \frac{2\alpha\psi}{\beta^2}\right)\right\}(1-e^{-\beta(t-t')}) \\ -\frac{r\psi}{\beta}(1-e^{-\beta(t-t')}) & e^{-\beta(t-t')} + \frac{r\alpha\psi}{\beta^2}(1-e^{-\beta(t-t')}) \end{pmatrix}. \tag{61}$$

For derivation and further details on the renormalized $\hat{\nu}$, refer to Verma [14]. The correlation matrix $\hat{C}(k,t-t')$ is given by

$$\begin{pmatrix} C^{++}(k,t,t') & C^{+-}(k,t,t') \\ C^{-+}(k,t,t') & C^{--}(k,t,t') \end{pmatrix} = \hat{G}(k,t-t') \begin{pmatrix} C^{++}(k) & C^{+-}(k) \\ C^{-+}(k) & C^{--}(k) \end{pmatrix} \tag{62}$$

The quantities $C^{\pm\pm}(k)$ can be written in terms of $E^{\pm}(k)$ as

$$C^{\pm\pm}(k) = \frac{2(2\pi)^d}{S_d(d-1)}k^{-(d-1)}E^{\pm}(k). \tag{63}$$

We take $C^{\pm\mp}(k) = 0$ (or $r_A = 1$) for simplifying the calculation. We take Kolmogorov's spectrum for $E^{\pm}(k)$ [see Eq. (52)], and

$$\hat{\nu}(k) = \begin{pmatrix} r\zeta & \alpha \\ r\psi & \beta \end{pmatrix} = \begin{pmatrix} r\zeta^* & \alpha^* \\ r\psi^* & \beta^* \end{pmatrix} \sqrt{K^+} \frac{(\Pi^+)^{2/3}}{(\Pi^-)^{1/3}}k^{-4/3} \tag{64}$$

The renormalized parameters $\zeta^*, \alpha^*, \psi^*$, and β^* have been calculated in Verma [14]. Finally, the matrices $\hat{G}(k,t-t')$ and $\hat{C}(k,t,t')$ can be written in in terms of renormalized parameters and Kolmogorov's spectrum.

Now we substitute $\hat{G}(k,t-t')$ and $\hat{C}(k,t,t')$ in Eq. (59), and keep terms only to the leading order in r. We find that the terms (1,4,5,8,9,10) of Eq. (59) vanish. The final equation for the fluxes $\Pi^{\pm}$ to the leading order in r are

$$\Pi^{\pm} = r\frac{(\Pi^+)^2}{\Pi^-}(K^+)^{3/2}\left[\frac{4S_{d-1}}{(d-1)^2 S_d}\int_0^1 dv \ln(1/v)\int_{1-v}^{1+v} dw(vw)^{d-2}(\sin\alpha)^{d-3}F^{\pm}(v,w)\right] \tag{65}$$

where the integrand $F^{\pm}$ are

$$\begin{aligned}
F^+ &= t_{13}(v,w)(vw)^{-d-2/3}\frac{1}{\beta^* w^{2/3}} + t_{14}(v,w)(vw)^{-d-2/3}\frac{\alpha^*}{\beta^*}\left\{\frac{1}{\beta^*(1+w^{2/3})} - \frac{1}{\beta^* w^{2/3}}\right\} \\
&+ t_{15}(v,w)w^{-d-2/3}\frac{1}{\beta^* w^{2/3}} + t_{16}(v,w)w^{-d-2/3}\frac{\alpha^*}{\beta^*}\left\{\frac{1}{\beta^*(v^{2/3}+w^{2/3})} - \frac{1}{\beta^* w^{2/3}}\right\} \\
&+ t_{17}(v,w)v^{-d-2/3}\frac{\alpha^*}{\beta^*}\left\{\frac{1}{\beta^*(v^{2/3}+w^{2/3})} - \frac{1}{\beta^* w^{2/3}}\right\} \\
&+ t_{18}(v,w)v^{-d-2/3}\frac{\alpha^*}{\beta^*}\left\{\frac{1}{\beta^*(1+w^{2/3})} - \frac{1}{\beta^* w^{2/3}}\right\} \tag{66}
\end{aligned}$$

$$F^- = t_{13}(v,w)(vw)^{-d-2/3}\frac{1}{\beta^*(1+v^{2/3})} + t_{15}(v,w)w^{-d-2/3}\frac{1}{\beta^*(1+v^{2/3})} \tag{67}$$

We denote the bracketed term of Eq. (65) by $I^{\pm}$ and compute them numerically. We find that the integrals are finite for $d = 2$ and 3. Also note that $I^{\pm}$ are independent of r. We calculate the constant $K^{\pm}$ of Eq. (65) in terms of $I^{\pm}$; the constants $K^{\pm}$ are listed in Table IV for various values of r in $d = 2$ and 3. The constants $K^{\pm}$ depend very sensitively on r. Also, there is a change of behaviour near $r = (I^-/I^+)^2 = r_c$; $K^- < K^+$ for $r < r_c$, whereas inequality reverses for r beyond r_c.

From the equations derived above, we can derive many important relationships. For example,

$$\frac{\Pi^-}{\Pi^+} = \frac{I^-}{I^+} \tag{68}$$

Since $I^{\pm}$ are independent of r, we can immediately conclude that the ratio Π^-/Π^+ is also *independent of* r. This is an important conclusion from our calculation. From the above equations we can also derive

$$K^+ = \frac{1}{r^{2/3}} \frac{(I^-)^{2/3}}{(I^+)^{4/3}} \tag{69}$$

$$K^- = r^{1/3} \frac{(I^+)^{2/3}}{(I^-)^{4/3}} \tag{70}$$

$$\frac{K^-}{K^+} = r \left(\frac{I^+}{I^-} \right)^2 \tag{71}$$

The total energy cascade rate can be written in terms of $E^+(k)$ as

$$\Pi = \frac{1}{2}(\Pi^+ + \Pi^-) = \frac{r}{2}(I^+ + I^-)(E^+(k))^{3/2}k^{5/2} \tag{72}$$

Since $I^{\pm}$ is independent of r, Π is a linear function of r. When we apply the above formula to the solar wind stream with $r = 0.07$, we find that $K^+ = 2.12$ and $K^- = 0.85$.

As mentioned in the previous section, the observed temperature evolution was studied by Verma *et al.* [25] and Tu [26]. For streams with $\sigma_c \to 1$, Verma *et al.* [25] had assumed that $K^+ = K^- = K$ independent of σ_c, and derived the total turbulent dissipation rate to be

$$\Pi = \frac{r + \sqrt{r}}{2K^{3/2}}(E^+(k))^{3/2}k^{5/2}. \tag{73}$$

Clearly the assumption that $K^+ = K^-$, as well as the above formula (73) is incorrect. Hence, the calculation of Verma *et al.* [25] needs to be modified. The substitution of the parameters r and $K^{\pm}$ in our formula (72) gives us an estimate of the turbulent heating that is an order of magnitude higher than the observed overall heating in the solar wind [25]. Some of the resolutions of this paradox are: (1) the assumption that the solar wind has reached steady-state is incorrect, and the formula (72) is inapplicable to the solar wind streams with large σ_c; or (2) the constants $K^{\pm}$ calculated above will be modified significantly by the mean magnetic field, anisotropy, and helicity etc. In case of the former, one needs to understand the nonequilibrium evolution of MHD turbulence, while in case of the latter, the field theoretic calculation has to generalized in presence of mean magnetic field and helicity. Both these generalizations are beyond the scope of this paper.

IV. SUMMARY AND CONCLUSIONS

In this paper we have theoretically calculated various energy cascade rates in the inertial range of *nonhelical* MHD turbulence. Our procedure is based on field-theoretic approach. Using the steady-state condition we also calculate the energy supply rate from the large-scale velocity field to the large-scale magnetic field. For simplicity of the calculation, we have taken two special cases: (1) $\sigma_c = 0$; (2) $\sigma_c \to 1$. Throughout the calculation we assume that the velocity modes at large length-scales are forced.

We will first summarize the results for $\sigma_c = 0$ case in $d = 3$. The cascade rates $\Pi_{b>}^{u<}$, $\Pi_{b>}^{b<}$, $\Pi_{b<}^{u<}$, $\Pi_{u>}^{b<}$ are approximately the same for r_A in the range of $0.5 - 1$, but the flux $\Pi_{u>}^{u<}$ is rather small. The sign of $\Pi_{b>}^{b<}$ is positive, indicating that the ME cascades forward, that is from large length-scales to small length-scales. The large-scale magnetic field is maintained by the $\Pi_{b<}^{u<}$ flux. We exploit this result to construct a dynamo model for galaxy. This result is discussed in paper II.

Recently Cho and Vishniac (CV) [21] performed numerical simulation of nonhelical MHD turbulence and arrived at the following conclusion based on their numerical results. In our language, their results for large r_A can be rephrased

as (1) $\Pi^{u<}_{u>} \approx U^3$; (2) $\Pi^{u<}_{(b<+b>)} \approx UB^2$; (3) $\Pi^{u<}_{b<} \approx (U - cB)B^2$, where U and B are the large-scale velocity and magnetic field respectively, and c is a constant. When we compare our theoretical findings with CV's result, we find our results can explain CV's first and second results, but they are only partly consistent with the third result. From Eq. (44) it can be easily seen that $\Pi^{u<}_{u>}$depends on the KE in the same manner as in fluid turbulence. Hence, $\Pi^{u<}_{u>} \approx U^3/L$, a result consistent with the first result of CV. Using $\Pi^{u<}_{(b<+b>)} = \Pi^{u<}_{b>} + \Pi^{b<}_{b>} + \Pi^{b<}_{u>}$ and the definitions of $F's$ [Eqs. (46-47)] we can easily show that

$$\frac{\Pi^{u<}_{(b<+b>)}}{\Pi} \approx ...r_A^{-1} + ...r_A^{-2} \tag{74}$$

where ... represents a constant. We estimate the above equation in the large r_A limit ($E^u \gg E^b$). In this limit, $\Pi \approx U^3/L$. Hence, to a leading order in r_A^{-1}

$$\Pi^{u<}_{(b<+b>)} \approx \Pi \frac{E^b}{E^u} \approx UB^2/L \tag{75}$$

From Eqs. (44-47), we also conclude that

$$\Pi^{u<}_{b<} \approx (...r_A^{-1} + ...r_A^{-2})\Pi \approx \left(...\frac{U}{L} - ...\frac{B^2}{UL}\right)B^2 \tag{76}$$

Note that the first part of the above equation matches with CV's first part, but the second part of $\Pi^{u<}_{b<}$ differs from CV's result by a factor of B/U. Since $B/U \approx 1$ at steady state, it is difficult to differentiate our results with that of CV. On the whole, our theoretical calculation is able to explain the numerical results of CV.

For $d = 3$ the Kolmogorov's constant K is approximately constant and is close to 1.5 for all r_A greater that $1/2$, same as that for fluid turbulence ($r_A = \infty$). This result implies that the total cascade rate does not change appreciably under the variation of r_A (since $\Pi \propto K^{-3/2}$). The cascade rates vanish near $r_A = 0.25$; this result is in the expected lines because MHD equations become linear in $r_A = 0$ limit. Comparison with the past results shows that our result differs from that of Verma and Bhattacharjee's calculation [31] where Kolmogorov's constant changes significantly with the variation of r_A. Note, however, that our procedure described here is an improvement over that of Verma and Bhattacharjee, where they had assumed a wavenumber cutoff for the self-energy integral for curing the infrared divergence problem. They had also assumed a specific type of self-energy matrix which can be shown to be correct only in some regime.

When we vary d, we find that for large d, $\Pi^{u<}_{u>} = \Pi^{u<}_{b>} = \Pi^{b<}_{b>} = \Pi^{b<}_{u>}$. In addition we also observe that Kolmogorov's constant MHD turbulence increases with dimensions as $d^{1/3}$. The same variation is observed for fluid turbulence [24]. This result indicates that the cascade rates decrease in higher dimensions. We could calculate fluxes for $d \geq 2.2$ because the RG fixed point is unstable for dimensions lower than 2.2 (Verma [14]). However, the RG fixed point for fluid turbulence is stable for $d = 2$, and the Kolmogorov's constant in the inverse cascade regime of 2D fluid turbulence comes out to be 6.3. For this computation, the renormalized viscosity ν^* was taken as -0.6. It is interesting to note that Dar et $al.$ [19] find negative KE flux ($\Pi^{u<}_{u>}$) in their 2D MHD turbulence simulation; this is reminiscent of 2D fluid turbulence.

In the other extreme limit $\sigma_c \to 1$ and $r_A = 1$, we find that Kolmogorov's constants K^+ and K^- are not equal, and the ratio K^-/K^+ depends very sensitively on $r = E^-(k)/E^+(k)$. Both the fluxes $\Pi^\pm$, and also the total flux Π, are proportional to r. The flux ratio Π^-/Π^+ is found to be independent of r. We also discuss the implications of our flux results to the heating of the solar wind.

In this paper we have restricted ourselves to nonhelical turbulence. Helical MHD turbulence is very important specially for the growth of magnetic energy (dynamo). The energy fluxes for helical MHD have been discussed in paper II. The study of the effects of mean magnetic field using field theory has been relegated for future.

APPENDIX A: VALUES OF T_i

The algebraic expressions for $T_i(k, p, q)$ are given below.

$$
\begin{aligned}
T_1(k, p, q) &= k_i P^+_{jab}(k) P_{ja}(p) P_{ib}(q) \\
&= kp \left((d-3)z + (d-2)xy + 2z^3 + 2xyz^2 + x^2 z \right) \quad (A1)
\end{aligned}
$$

$$
\begin{aligned}
T_3(k, p, q) &= k_i P^-_{jab}(k) P_{ja}(p) P_{ib}(q) \\
&= -k^2 \left((d-2)(1-y^2) + z^2 + xyz \right) \quad (A2)
\end{aligned}
$$

$$
\begin{aligned}
T_5(k, p, q) &= -k_i P^+_{jab}(p) P_{ja}(k) P_{ib}(q) \\
&= -kp \left((d-3)z + (d-2)xy + 2z^3 + 2xyz^2 + y^2 z \right) \quad (A3)
\end{aligned}
$$

$$
\begin{aligned}
T_7(k, p, q) &= -k_i P^-_{jab}(p) P_{ja}(k) P_{ib}(q) \\
&= -kp \left((2-d)xy + (1-d)z + y^2 z \right) \quad (A4)
\end{aligned}
$$

$$
\begin{aligned}
T_9(k, p, q) &= -k_i P^+_{iab}(q) P_{ja}(k) P_{jb}(p) \\
&= -kq \left(xz - 2xy^2 z - yz^2 \right) \quad (A5)
\end{aligned}
$$

$$
\begin{aligned}
T_{11}(k, p, q) &= -k_i P^-_{iab}(q) P_{ja}(k) P_{jb}(p) \\
&= -kqz \left(x + yz \right) \quad (A6)
\end{aligned}
$$

$$
T_{2n}(k, p, q) = -T_{2n-1}(k, p, q) \qquad \text{for } n = 1..6 \quad (A7)
$$

$$
\begin{aligned}
T_{13,15}(k, p, q) &= k_i M_{jab}(k') P_{ja}(p) P_{ib}(q) \\
&= -kpyz(y + xz) \quad (A8)
\end{aligned}
$$

$$
\begin{aligned}
T_{14,16}(k, p, q) &= k_i M_{jab}(k') P_{jb}(p) P_{ia}(q) \\
&= k^2(1-y^2)(d-2+z^2) \quad (A9)
\end{aligned}
$$

$$
\begin{aligned}
T_{17,19}(k, p, q) &= k_i M_{jab}(p) P_{ja}(k) P_{ib}(q) \\
&= kpxz(x + yz) \quad (A10)
\end{aligned}
$$

$$
T_{18,20}(k, p, q) = -T_{14}(k, p, q) \quad (A11)
$$

$$
\begin{aligned}
T_{21,23}(k, p, q) &= k_i M_{iab}(q) P_{ja}(k) P_{jb}(p) \\
&= -kpxy(1 - z^2) \quad (A12)
\end{aligned}
$$

$$
T_{22,24}(k, p, q) = -T_{13}(k, p, q) \quad (A13)
$$

where $\mathbf{k} = \mathbf{p} + \mathbf{q}$, and x, y, z are defined by

$$
\mathbf{p} \cdot \mathbf{q} = -pqx; \qquad \mathbf{q} \cdot \mathbf{k} = qky; \qquad \mathbf{p} \cdot \mathbf{k} = pkz. \quad (A14)
$$

[1] R. H. Kraichnan, Phys. Fluids **8**, 1385 (1965).
[2] P. S. Iroshnikov, Sov. Astron. I. **7**, 566 (1964).
[3] E. Marsch, in *Reviews in Modern Astronomy*, edited by G. Klare (Springer-Verlag, Berlin, 1990), p. 43.
[4] W. H. Matthaeus and Y. Zhou, Phys. Fluids B **1**, 1929 (1989).
[5] Y. Zhou and W. H. Matthaeus, J. Geophys. Res. **95**, 10291 (1990).
[6] M. K. Verma *et al.*, J. Geophys. Res. **101**, 21619 (1996).
[7] P. Frick and D. Sokoloff, Phys. Rev. E **57**, 4155 (1998).
[8] W. C. Müller and D. Biskamp, Phys. Rev. Lett. **84**, 475 (2000).
[9] D. Biskamp and W. C. Müller, Phys. Plasma **7**, 4889 (2000).
[10] M. K. Verma, Phys. Plasma **6**, 1455 (1999).
[11] S. Sridhar and P. Goldreich, Astrophys. J. **432**, 612 (1994).
[12] P. Goldreich and S. Sridhar, Astrophys. J. **438**, 763 (1995).
[13] M. K. Verma, Phys. Rev. E **64**, 26305 (2001).
[14] M. K. Verma, Phys. Plasma **8**, 3945 (2001).
[15] M. Hnatich, J. Honkonen, and M. Jurcisin, nlin.CD/0106043 (2001).
[16] A. Pouquet, U. Frisch, and J. Léorat, J. Fluid Mech. **77**, 321 (1976).
[17] A. Pouquet and G. S. Patterson, J. Fluid Mech. **85**, 305 (1978).

[18] M. K. Verma, Pramana (submitted), nlin.CD/0107069 (2002).

[19] G. Dar, M. K. Verma, and V. Eswaran, Physica D **157**, 207 (2001).

[20] A. Ishizawa and Y. Hattori, J. Phy. Soc. Jpn. **67**, 441 (1998).

[21] J. Cho and E. T. Vishniac, Astrophys. J. **538**, 217 (2000).

[22] M. M. Stanišić, *Mathematic Theory of Turbulence* (Springer-Verlag, New York, 1988).

[23] D. C. Leslie, *Development in the Theory of Turbulence* (Claredon, Oxford University Press, 1973).

[24] J. D. Fournier and U. Frisch, Phys. Rev. A **17**, 747 (1979).

[25] M. K. Verma, D. A. Roberts, and M. L. Goldstein, J. Geophys. Res. **100**, 19839 (1995).

[26] C.-Y. Tu, J. Geophys. Res. **93**, 7 (1988).

[27] M. K. Verma, Int. J. Mod. Phy. B (submitted), nlin.CD/0103033 (2001).

[28] G. Dar, Ph.D. thesis, I. I. T. Kanpur, 2000.

[29] W. H. Matthaeus and M. L. Goldstein, J. Geophys. Res. **87**, 6011 (1982).

[30] E. Marsch and C.-Y. Tu, J. Geophys. Res. **95**, 8211 (1990).

[31] M. K. Verma and J. K. Bhattacharjee, Europhys. Lett. **31**, 195 (1995).

Figure Captions

Fig. 1. Various energy cascade rates of MHD turbulence. The illustrated wavenumber spheres contain $\mathbf{u} <$ and $\mathbf{b} <$ modes, while $\mathbf{u} >$ and $\mathbf{b} >$ are modes outside these spheres. The velocity fields is forced at large-scale.

TABLE I: The flux ratios computed by Dar *et al.* ($d = 2, \sigma_c \approx 0, r_A \approx 0.5$)

$\Pi_{u>}^{u<}/\Pi$	$\Pi_{b>}^{u<}/\Pi$	$\Pi_{u>}^{b<}/\Pi$	$\Pi_{b>}^{b<}/\Pi$	$\Pi_{b<}^{u<}/\Pi$	K^+
-0.13	0.68	-0.09	0.47	0.37	≈ 4

TABLE II: The computed values of energy cascade rates of MHD turbulence for various r_A when $\mathbf{d = 3}$ and $\sigma_c = 0$.

$\Pi \setminus r_A$	5000	100	5	1	0.5	0.3	Trend
$\Pi_{u>}^{u<}/\Pi$	1	0.97	0.60	0.12	0.037	0.011	decreases
$\Pi_{b>}^{u<}/\Pi$	3.5E-4	1.7E-2	0.25	0.40	0.33	0.36	increases then saturates
$\Pi_{u>}^{b<}/\Pi$	-1.1E-4	-5.1E-3	-0.05	0.12	0.33	0.42	increases then saturates
$\Pi_{b>}^{b<}/\Pi$	2.7E-4	1.3E-2	0.20	0.35	0.30	0.21	increases then dips
$\Pi_{b<}^{u<}/\Pi$	1.7E-4	8.1E-3	0.15	0.47	0.63	0.63	increases then saturates
K^+	1.53	1.51	1.55	1.50	1.65	3.26	approx. const till $r_A \approx 0.5$
K^u	1.53	1.50	1.29	0.75	0.55	0.75	decreases

TABLE IV: The computed values Kolmogorov's constants for $\sigma_c \to 1$ and $r_A = 1$ limit for various $r = E^-/E^+$ ($d = 2, 3$)

d	r	K^+	K^-
	0.17	1.4	1.4
	0.10	2.1	1.2
3	0.07	2.7	1.07
	10^{-3}	45	0.26
	10^{-6}	4528	0.026
	0.1	1.2	2.4
	0.07	1.5	2.2
2	0.047	1.9	1.9
	10^{-3}	25	0.52
	10^{-6}	2480	0.052

TABLE III: The computed values of energy cascade rates of MHD turbulence for various space dimensions d when $\sigma_c = 0$ and $r_A = 1$.

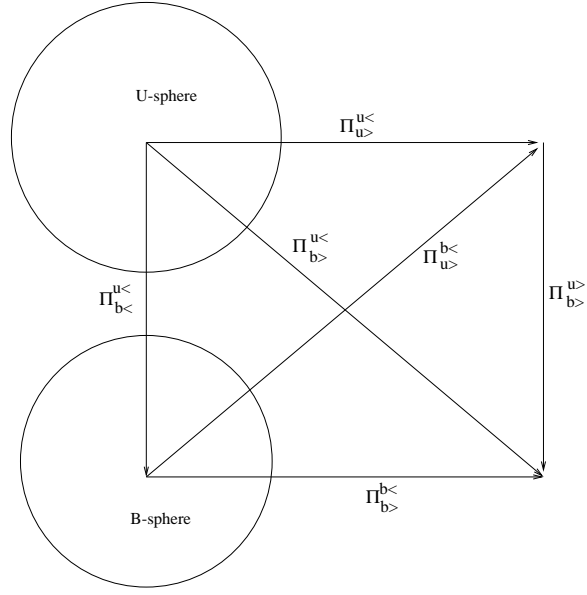| $\Pi \setminus d$	2.1	2.2	2.5	3	4	10	100
$\Pi_{u>}^{u<}/\Pi$	-	0.02	0.068	0.12	0.17	0.23	0.25
$\Pi_{b>}^{u<}/\Pi$	-	0.61	0.49	0.40	0.34	0.27	0.25
$\Pi_{u>}^{b<}/\Pi$	-	-0.027	0.048	0.12	0.18	0.23	0.25
$\Pi_{b>}^{b<}/\Pi$	-	0.40	0.39	0.35	0.31	0.27	0.25
$\Pi_{b<}^{u<}/\Pi$	-	0.37	0.4	0.47	0.49	0.50	0.50
K^+	-	1.4	1.4	1.50	1.57	1.90	3.46
K^u	-	0.69	0.72	0.75	0.79	0.95	1.73

FIG. 1: Various energy cascade rates of MHD turbulence. The illustrated wavenumber spheres contain $\mathbf{u}<$ and $\mathbf{b}<$ modes, while $\mathbf{u}>$ and $\mathbf{b}>$ are modes outside these spheres. The velocity fields is forced at large-scale.